Violet Grove 2D data processing at CREWES update

Han-xing Lu, Kevin W. Hall and Don C. Lawton

ABSTRACT

A series of 3C-2D seismic lines were simultaneously acquired in 2005 by Veritas DGC Inc. in the Pembina field near Violet Grove, Alberta. These data are the baseline survey for a 4D study, intended to monitor reservoir changes during ongoing CO_2 injection. Lines 1, 4 and 5 were oriented N-S (lines 4 and 5 are receiver lines), and lines 2 and 3 are E-W lines. A previous report has discussed CREWES processing of line 1 as a 2D line, and all lines as a 3D volume.

This update details vertical and radial component processing of lines 2 and 3, with an emphasis on radial component processing. Data quality is high, and good results have been obtained for these lines, which are very comparable to earlier results from CREWES and Veritas.

INTRODUCTION

Two E-W and three N-S 3C-2D seismic lines were acquired in 2005 by Veritas DGC Inc. in the Pembina Field near Violet Grove, Alberta (Figure 1). An overview of this project has been provided by Lawton et al. (2005). Lines 1-3 are source and receiver lines, lines 4 and 5 are receiver lines only. All receivers were live for all shots. Initial 2D processing of Line 1 and 3D processing of all lines has previously been reported by Lu et al. (2005). This report details 2D processing of lines 2 and 3 from the Violet Grove baseline survey at CREWES, with an emphasis on radial component processing
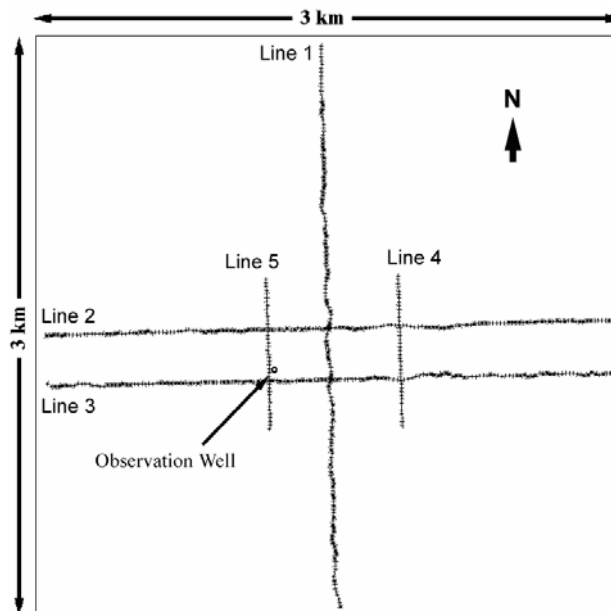

FIG. 1. Survey geometry (from Lu et al., 2005). Lines 2 and 3 processed as 2D lines are discussed in this report.

3C-2D PROCESSING

Lines 2 and 3 have been processed following flows originally presented by Lu and Margrave (1998; Table 1), and detailed by Lu and Hall (2003).

Table 1. Vertical (left) and radial (right) processing flows (Lu and Margrave, 1998).

TRACE EDIT	TRACE EDIT
TRUE AMPLITUDE RECOVERY	ASYMPTOTIC BINNING
SURFACE CONSISTENT DECONVOLUTION	SURFACE CONSISTENT DECONVOLUTION
TIME VARIANT SPECTRAL WHITENING	TIME VARIANT SPECTRAL WHITENING
ELEVATION AND REFRACTION STATIC CORRECTIONS	ELEVATION STATICS
VELOCITY ANALYSIS	APPLY FINAL REFRACTION AND RESIDUAL STATICS FROM P-P
RESIDUAL SURFACE CONSISTENT STATICS	CONSTRUCT INITIAL P-SV VELOCITY FROM FINAL P-P VEL.
NORMAL MOVEOUT	VELOCITY ANALYSIS
TRIM STATICS	RECEIVER RESIDUAL STATICS (HAND STATICS)
FRONT END MUTING	VELOCITY ANALYSIS
CDP STACK	CONVENTIONAL RESIDUAL STATICS
TIME VARIANT SPECTRAL WHITENING	VELOCITY ANALYSIS
TRACE EQUALIZATION	NORMAL MOVEOUT
F-XY DECONVOLUTION	ACP TRIM STATICS
3D PHASE-SHIFT MIGRATION	FRONT END MUTING
FOR TRACE DISPLAY:	ACP STACK (DEPTH-VARIANT STACK AND DMO STACK)
TRACE EQUALIZATION	TIME VARIANT SPECTRAL WHITENING
BANDPASS FILTER	TRACE EQUALIZATION
TIME VARIANT SCALING	F-XY DECONVOLUTION
	3D PHASE-SHIFT MIGRATION
	FOR TRACE DISPLAY:
	TRACE EQUALIZATION
	BANDPASS FILTER
	TIME VARIANT SCALING

Orientation

The data for lines 2 and 3 were extracted from field records (all receivers live for all shots), and separated into vertical (V) and horizontal components (H1 and H2; Figure 2). Lines 2 and 3 have a bearing of 268° from geographic North, but the geophones were planted with H1 oriented towards magnetic North (~20° difference). So, a component rotation must be performed in order to obtain the radial (R) and transverse (T) components. For initial processing, a simple 2C geometric rotation was performed, which assumes that the geophones were planted vertically and particle motion of incident wave-fronts is precisely vertical or horizontal (Figure 3).

Inspection of the results shows that reflection energy has been enhanced on R, and decreased on T (Blue ovals; Figure 2 and 3). Also, trace polarity is reversed on the trailing spread of R, but not on T (Figure 4). Since these are the expected results, we accepted these R and T component shot gathers for further processing.
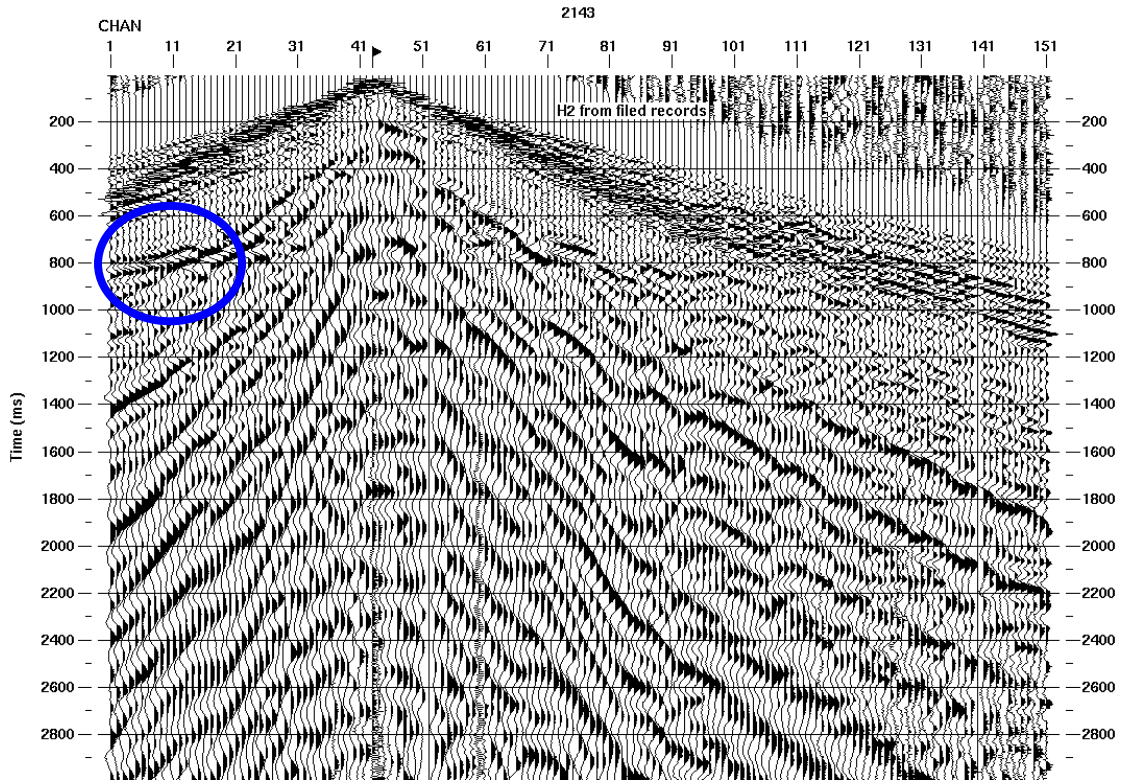
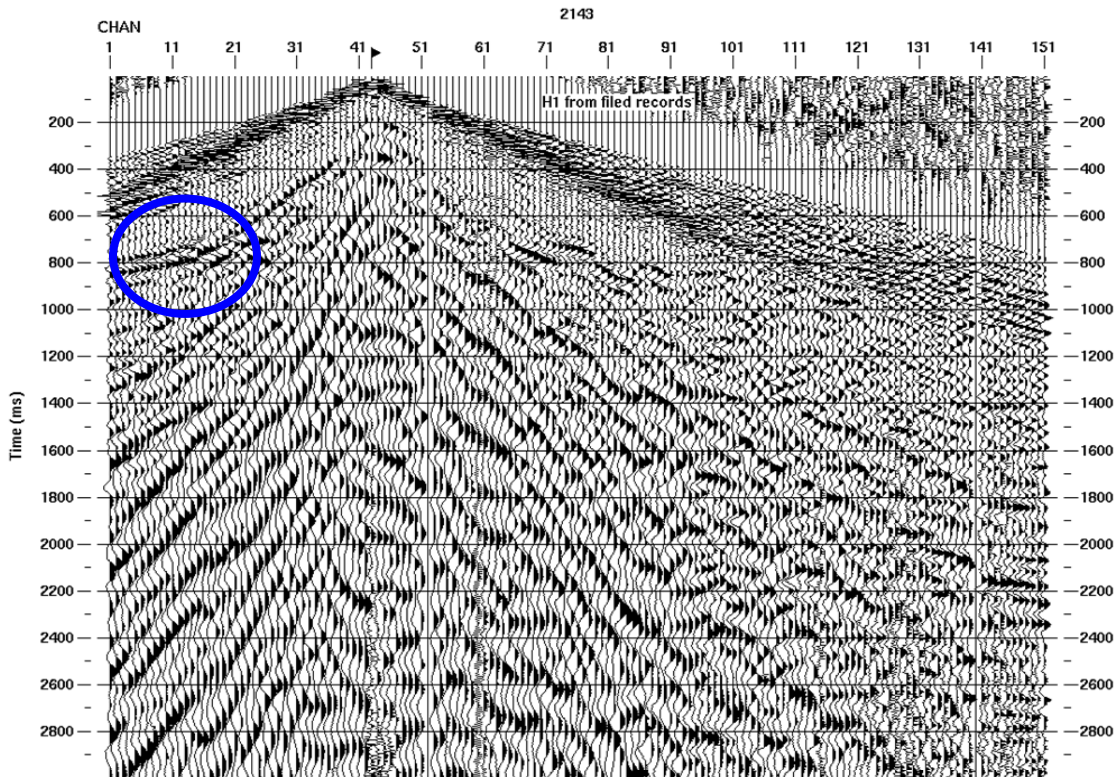FIG. 2a. Line 2; H2 shot gather (closest to radial before component rotation).

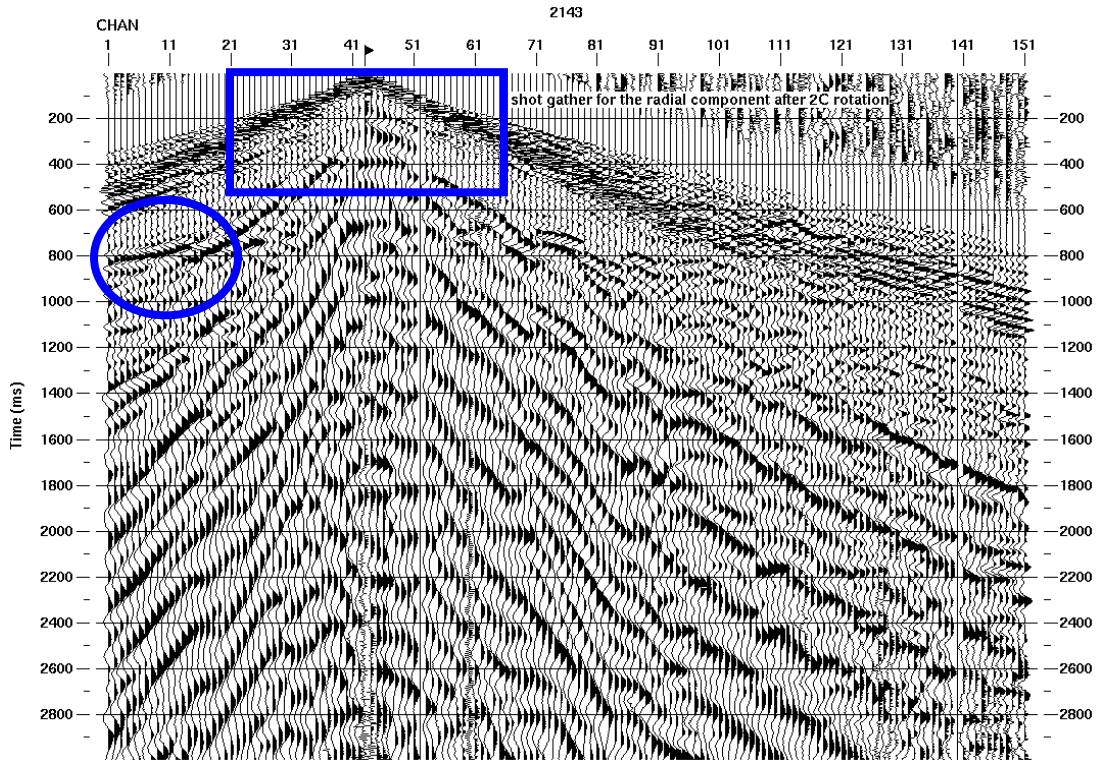FIG. 2b. Line 2; H1 shot gather (closest to transverse before component rotation).

FIG. 3a. Line 2; Radial component shot gather after 2C geometric rotation. Rectangle shows location of Figure 4a.
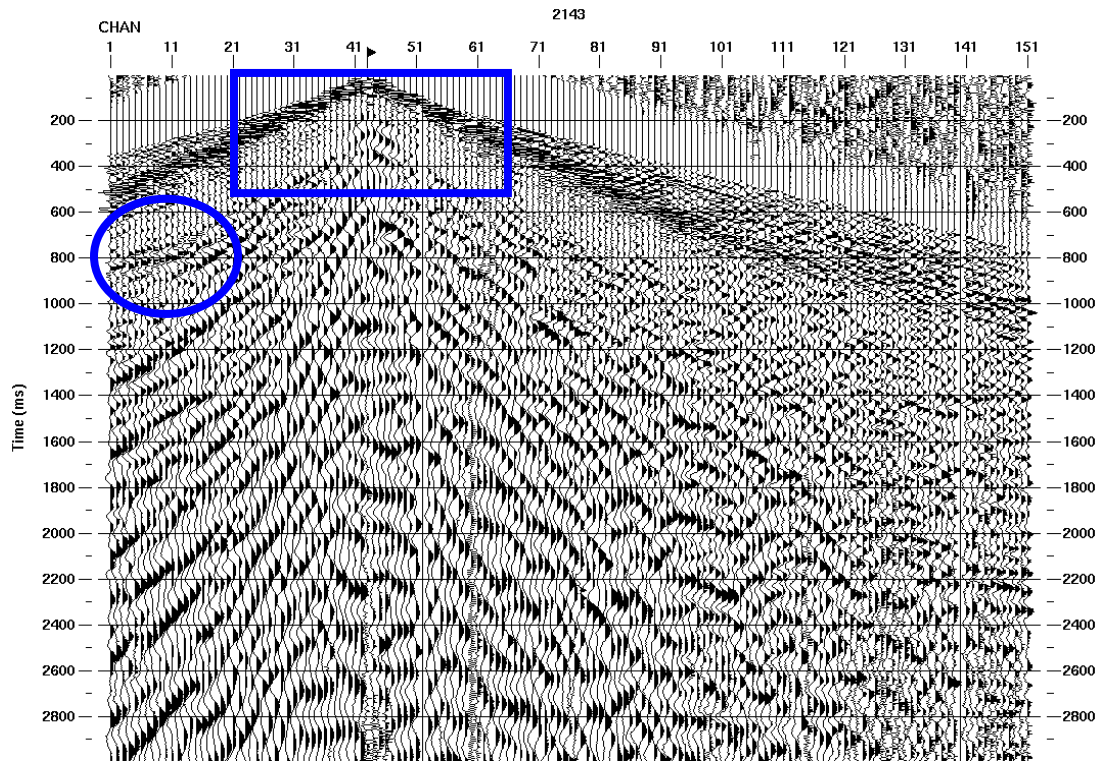

FIG. 3b. Line 2; Transverse component shot gather after 2C geometric rotation. Rectangle shows location of Figure 4b.
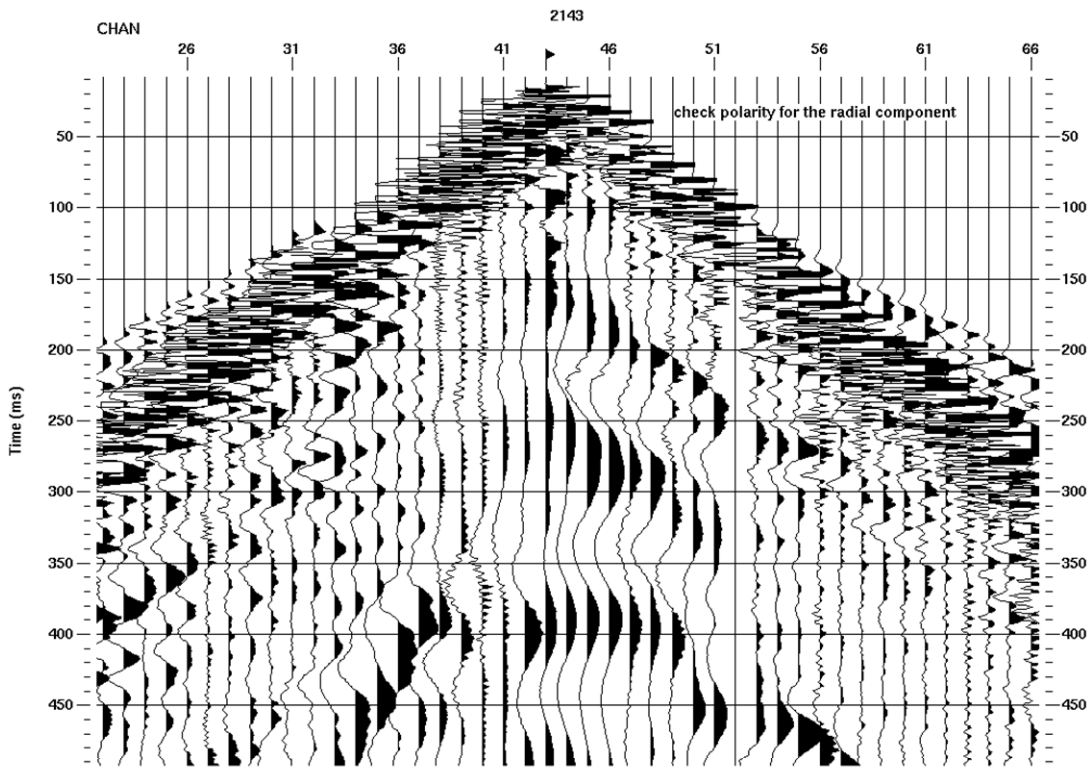
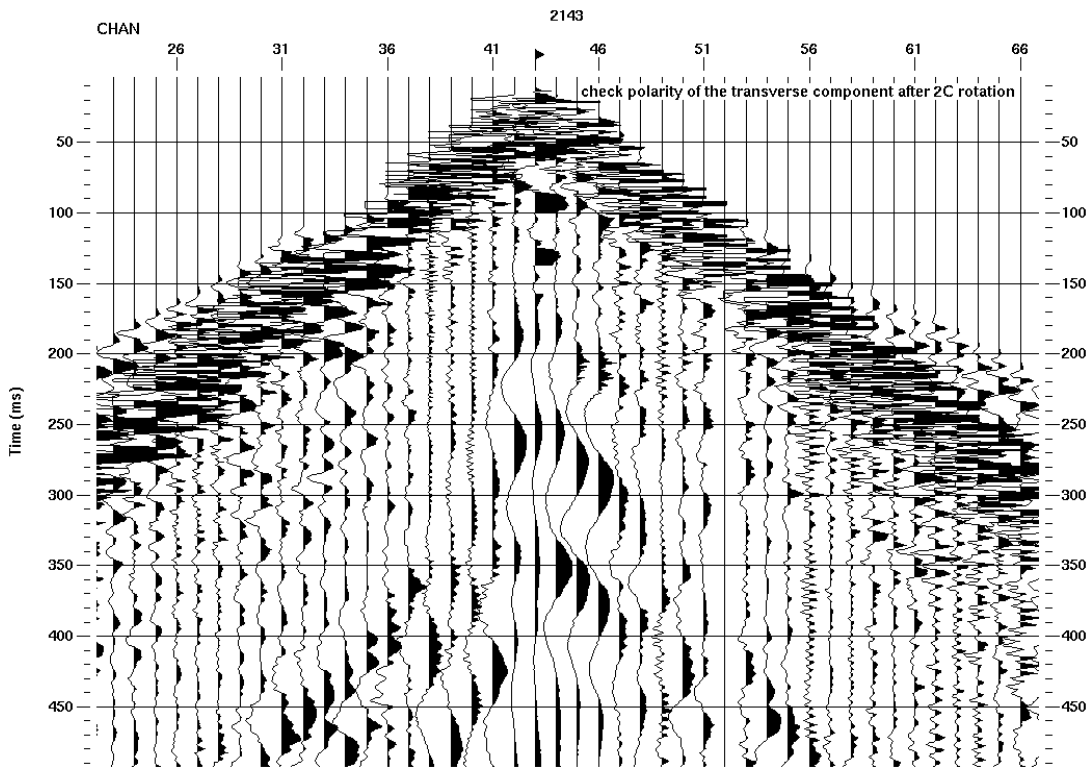FIG. 4a. Line 2; Radial component shot gather. Note polarity reversal on the trailing spread.

FIG. 4b. Line 2; Transverse component shot gather. Trace polarity is not reversed on the trailing spread.

Radial component noise attenuation

As shown in Figure 5a, the R component shot gathers (also called P-S) contain a large amount of surface-wave noise, which over-powers any signal that may be present. On the vertical component (P-P), much of this low-frequency noise can be attenuated with a bandpass filter. This method is less appropriate for P-S data, since noise and signal frequencies overlap to a much greater extent. The ProMAX surface-wave noise attenuation module, which uses a low-frequency array forming method, was used to produce the result shown in Figure 5b.

Statics

A weathering layer P-wave velocity of 610 m/s, final datum of 904.5 m, and replacement velocity of 3450 m/s were used for P-P statics. The weathering layer velocity is one that has worked well in the past (typically in the 600-900 m/s range), final datum is the maximum elevation of the survey, and replacement velocity is the highest sub-weathering velocity calculated from the vertical component shot gathers.

P-S receiver statics are difficult to calculate, because they are affected by near-surface shear-wave velocities which tend to have large lateral variations. Typically, statics are hand-picked from receiver stacks created using P-P shot statics, a P-S velocity function calculated from P-P velocities, and P-P receiver statics scaled by a constant V_P/V_S ratio (Figure 6a). In this case, the P-S data quality is high enough that semblance-based velocity picking could be successfully performed on asymptotic conversion point (ACP) gathers. This velocity function results in a significantly improved receiver stack to use as a starting point for hand statics (Figure 6b). Figure 6c shows the receiver stack after application of two rounds of hand-picked P-S receiver statics.

Maximum migration angle

Most migration modules have a default maximum migration angle of 90 degrees. However, this is not necessary in areas with little to no geologic structure. Figure 7 shows a comparison of phase-shift migrations performed on the Line 2 P-P stack. A maximum angle of 90 degrees results in a noisier, less interpretable, migrated section.

Source-receiver offset range

We often present offset-limited stacks, primarily to attenuate source-generated noise at near-offsets. Figure 8 shows P-S migrated sections containing offsets from 0-2500 m (Figure 8a) and 150-2500 m (Figure 8b). Exclusion of near-offsets in the 0-150 m range results in a cleaner section, with improved reflection continuity. We can safely exclude these near-offsets in this case, because we are interested in a deep target (~1600 m). Vertical component stacks shown in this report have an offset range of 20-1900 m
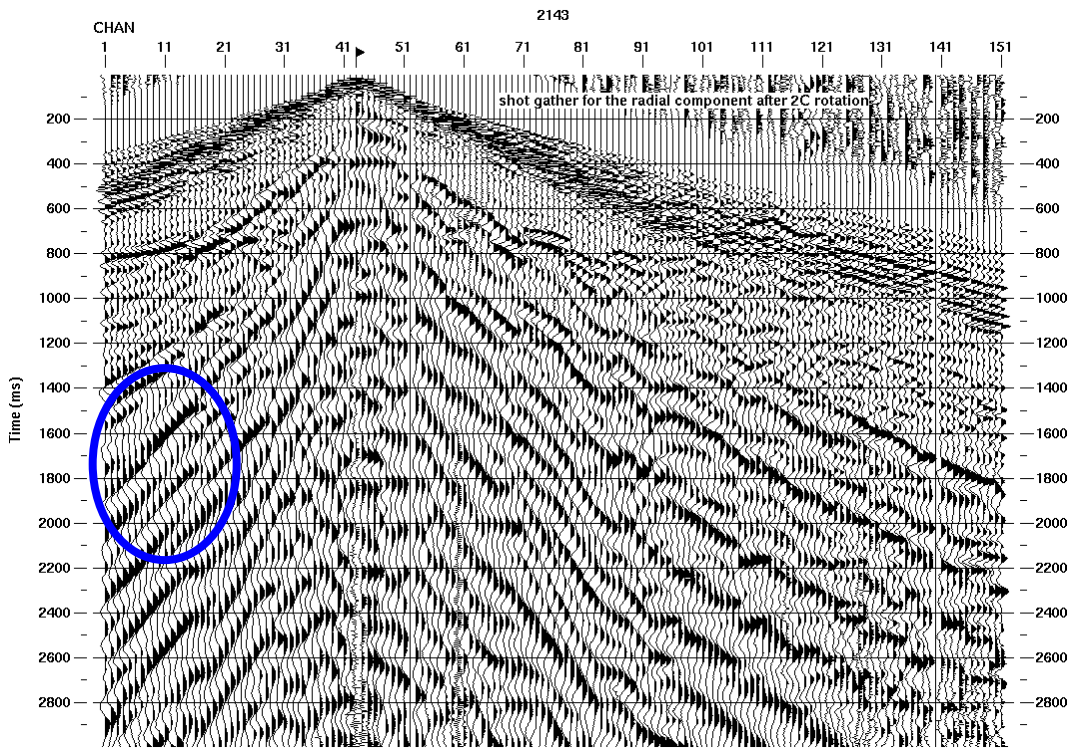
FIG. 5a Line 2; P-S shot gather after 2C geometric rotation (Copy of Figure 3a).
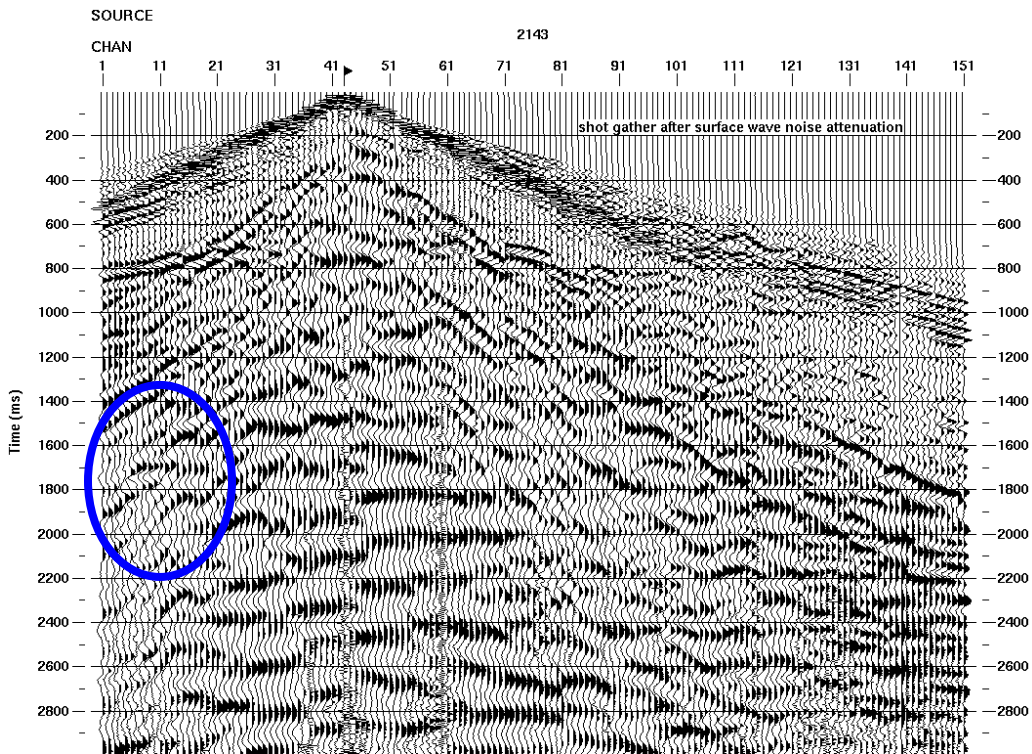

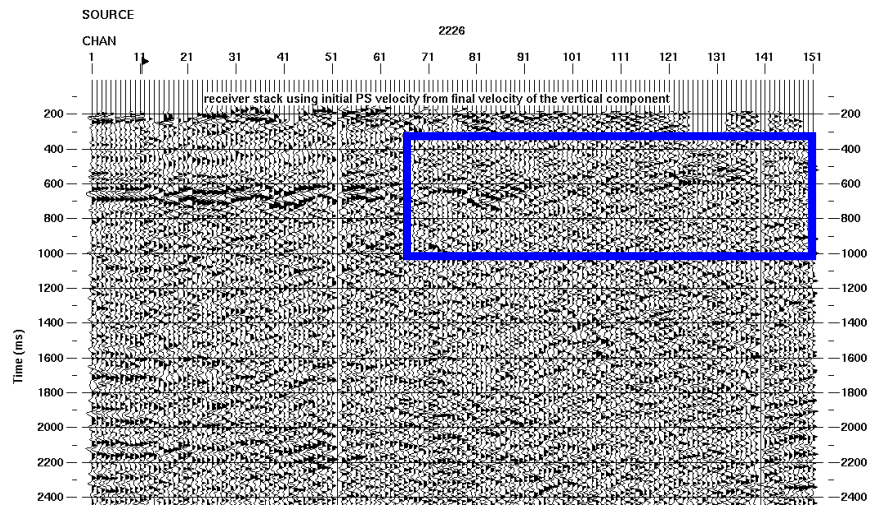FIG. 5b. Line 2; Figure 5a after surface wave noise attenuation.

FIG. 6a. Line 2; P-S receiver stack using P-S velocity function calculated from P-P velocities.
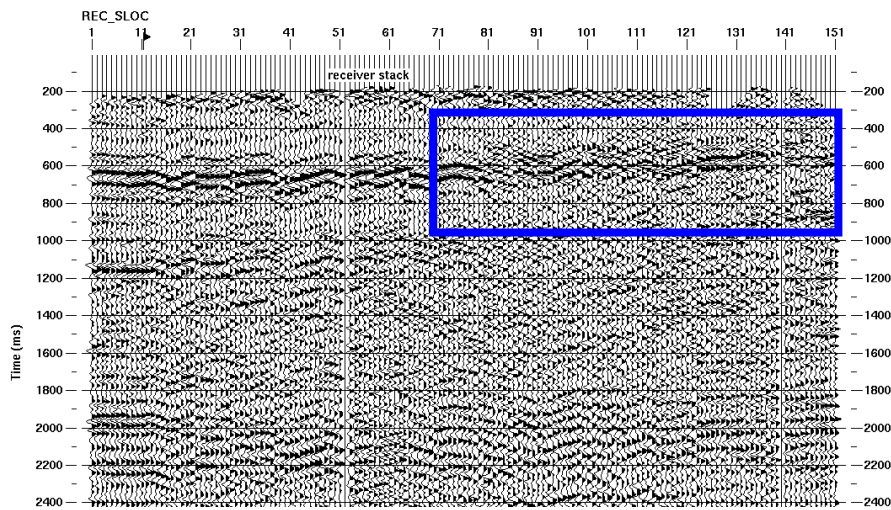

FIG. 6b. Line 2; P-S receiver stack with P-S velocity function picked from ACP gathers.
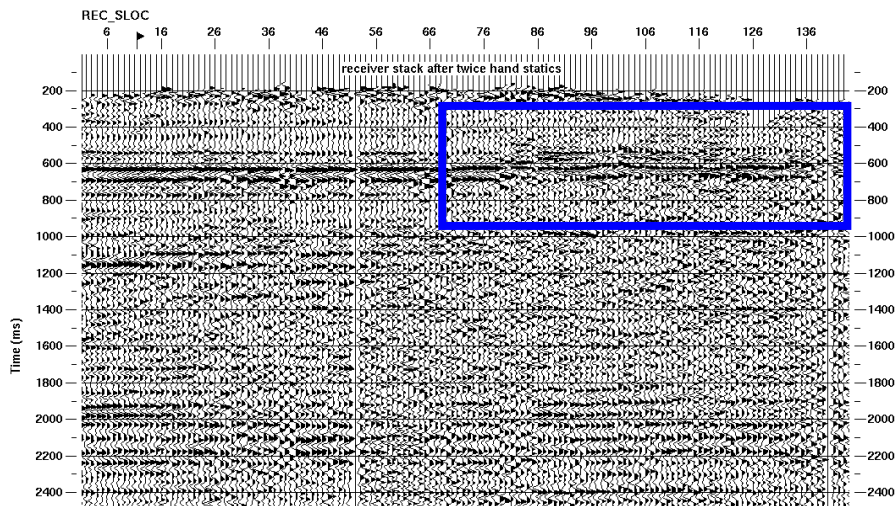

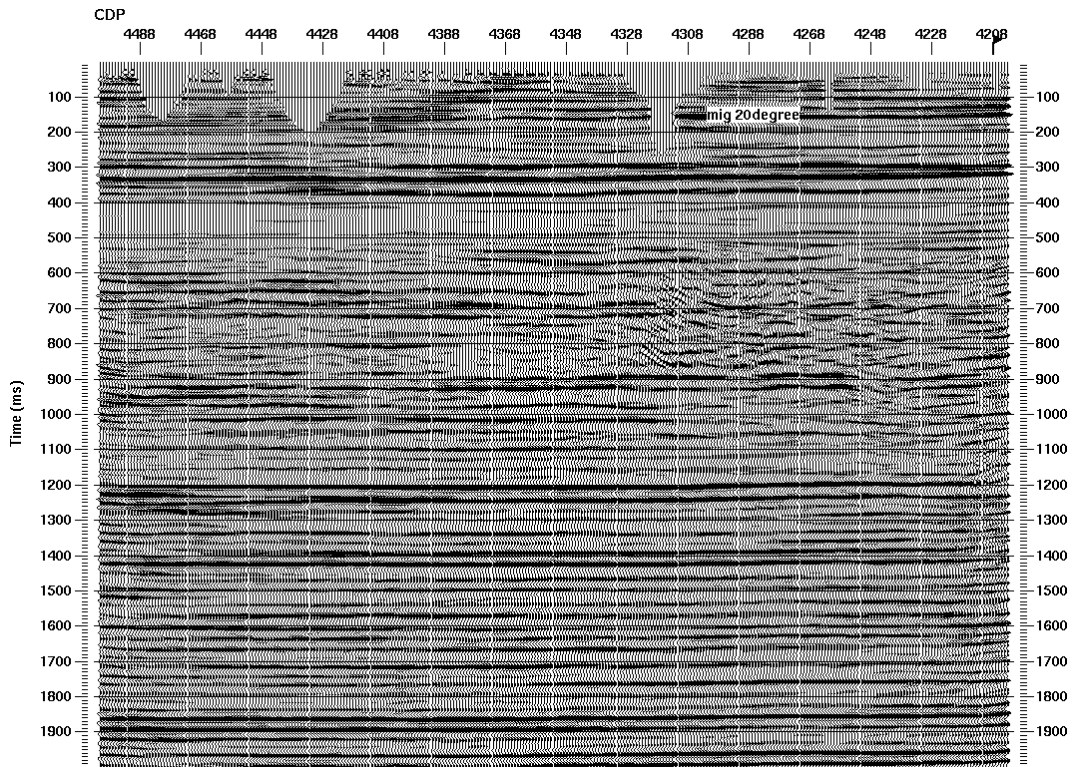FIG. 6c. Line 2; P-S receiver stack after application of receiver hand statics to Figure 6b.

FIG. 7a. Line 2; P-P phase-shift migrated stack with a 20 degree maximum migration angle.
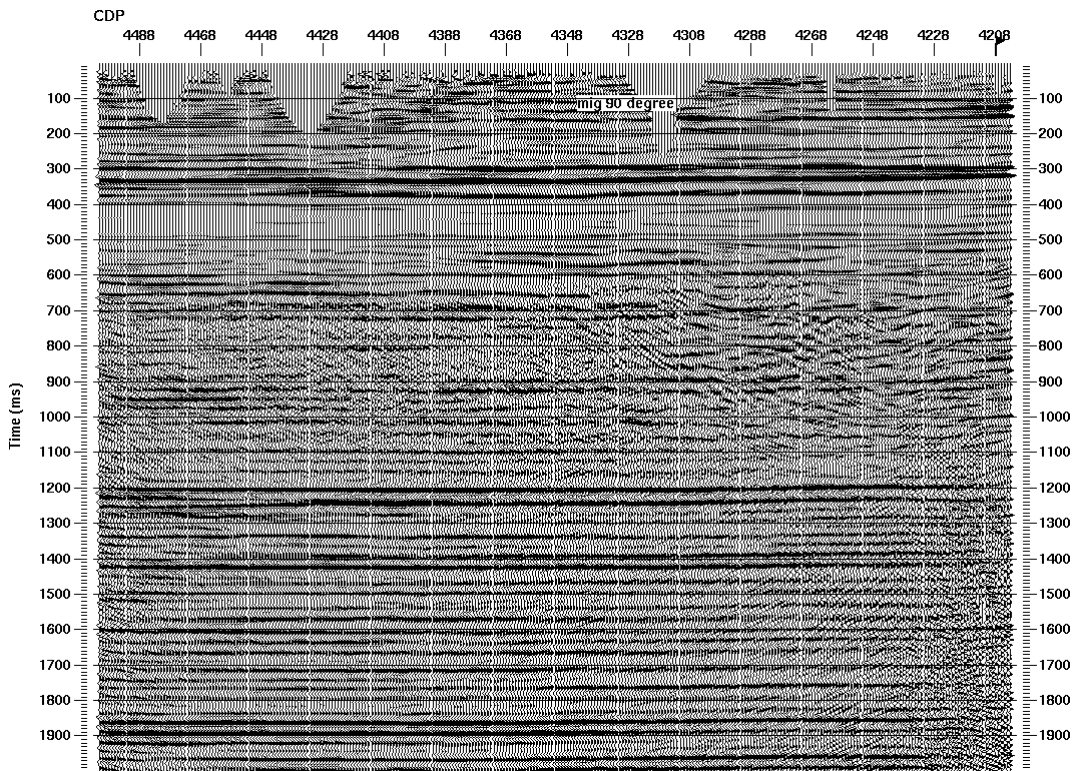
FIG. 7b. Line 2; P-P phase-shift migrated stack with a 90 degree maximum migration angle.
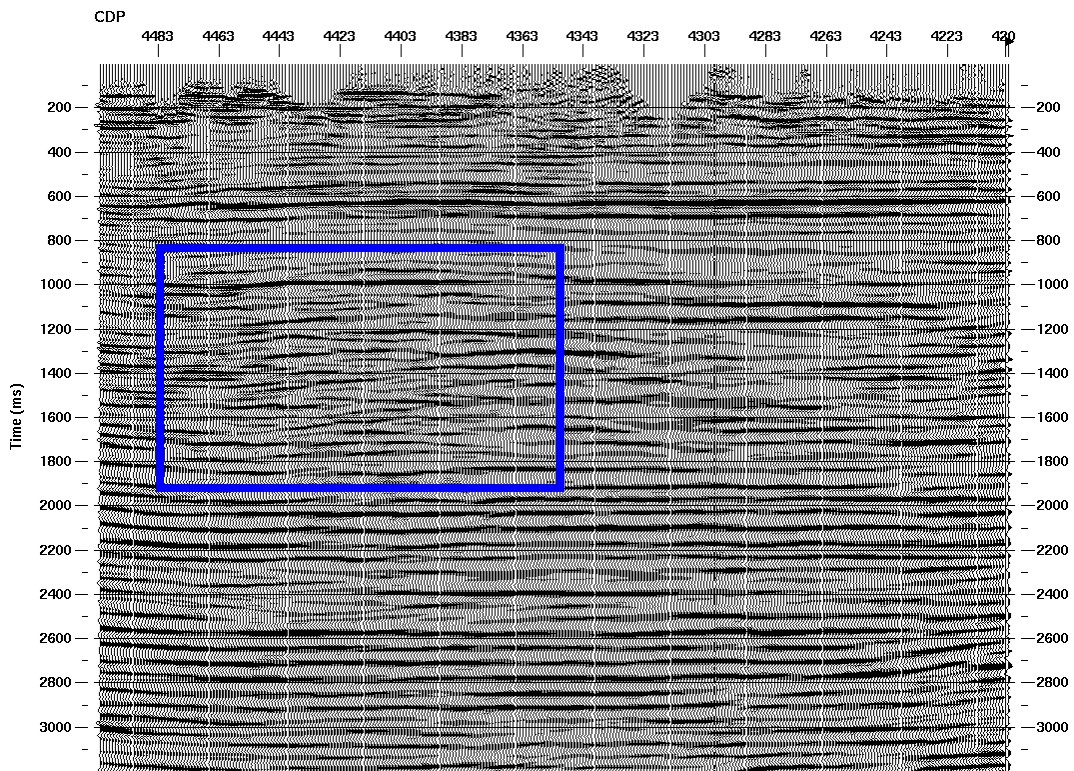
FIG. 8a. Line 2; P-S migrated section, 0-2500 m offsets.
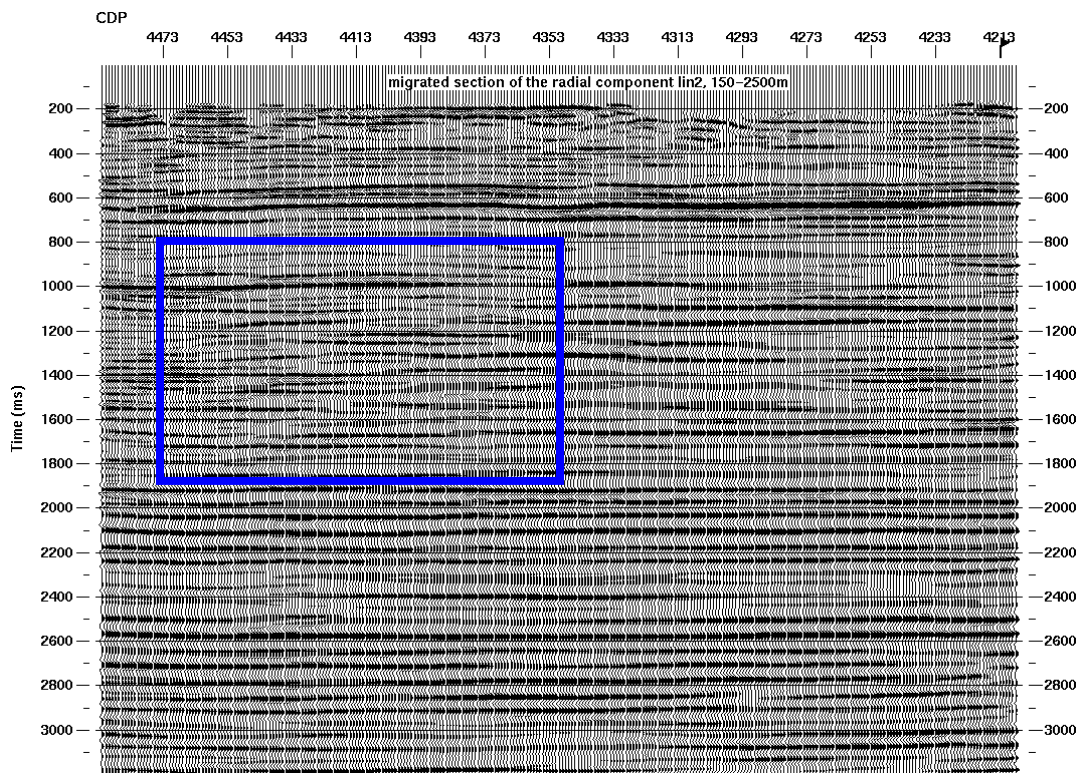
FIG. 8b. Line 2; P-S migrated section, 150-2500 m

Final results

Final migrated P-P and P-S results are shown in Figures 9 and 10. All stacks shown have been bandpass filtered (100 Hz max) and had AGC applied for display. If the P-S travel-times are scaled by 1.5 (equivalent to a V_P/V_S of 2.0) and compared to the P-P section, the reflections match quite well (Figure 11). A comparison of radial to transverse sections shows little to no correspondence, as expected in the absence of anisotropy (not shown). This implies that the radial component results are reliable.

There is also good correspondence between the 2D sections and earlier 3D volumes obtained from the same data (Figure 12). Figure 13 shows a comparison of CREWES results to a section processed by Veritas. The contractor section contains higher amplitudes between 50 and 100 Hz, but less reflection continuity, possibly as a result (blue circles, Figure 13). Spectral whitening tests were conducted for several frequency ranges (4-8-220-240 Hz, 4-8-120-140 Hz, 4-8-100-120 Hz). No significant differences were observed, which implies that higher frequencies are mostly noise, which stacks out.
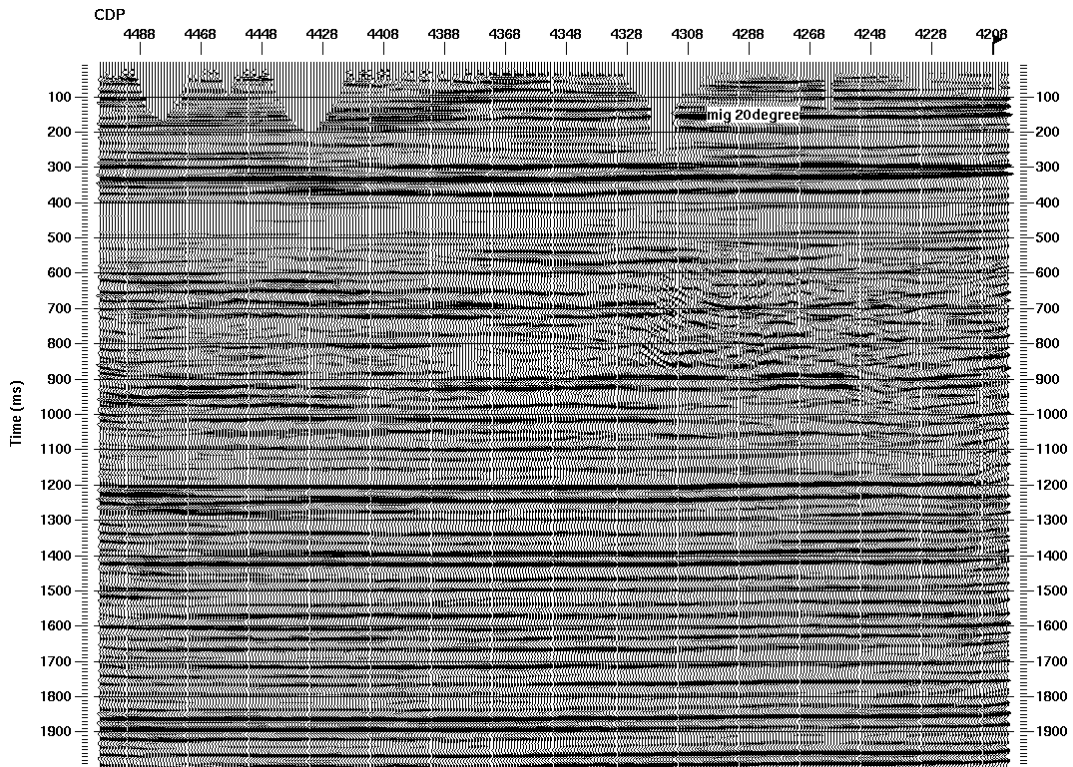
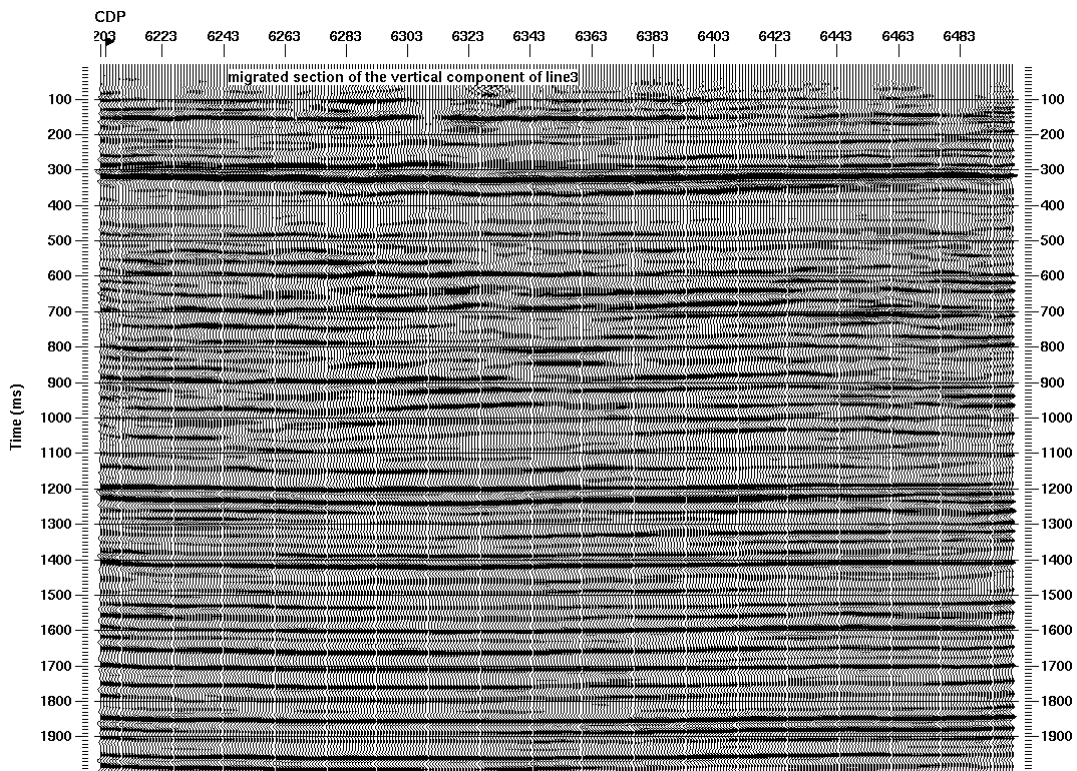FIG. 9a. Line 2; Final migrated P-P section.
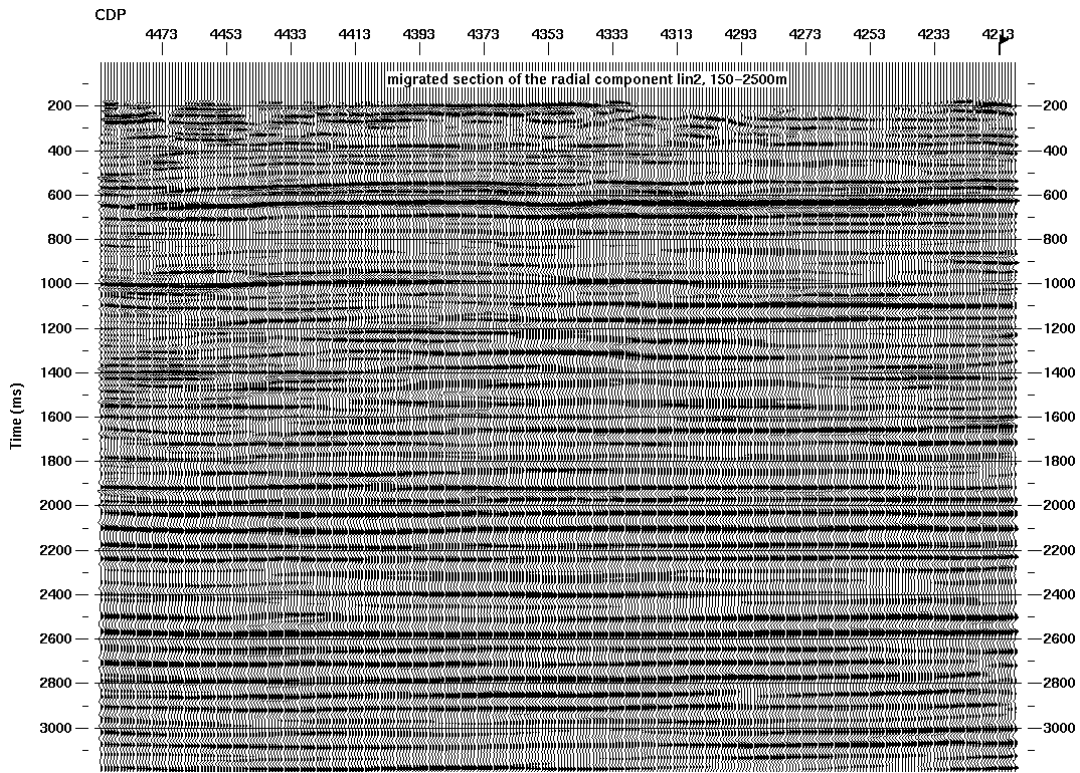
FIG. 9b. Line 3; Final migrated P-P section.

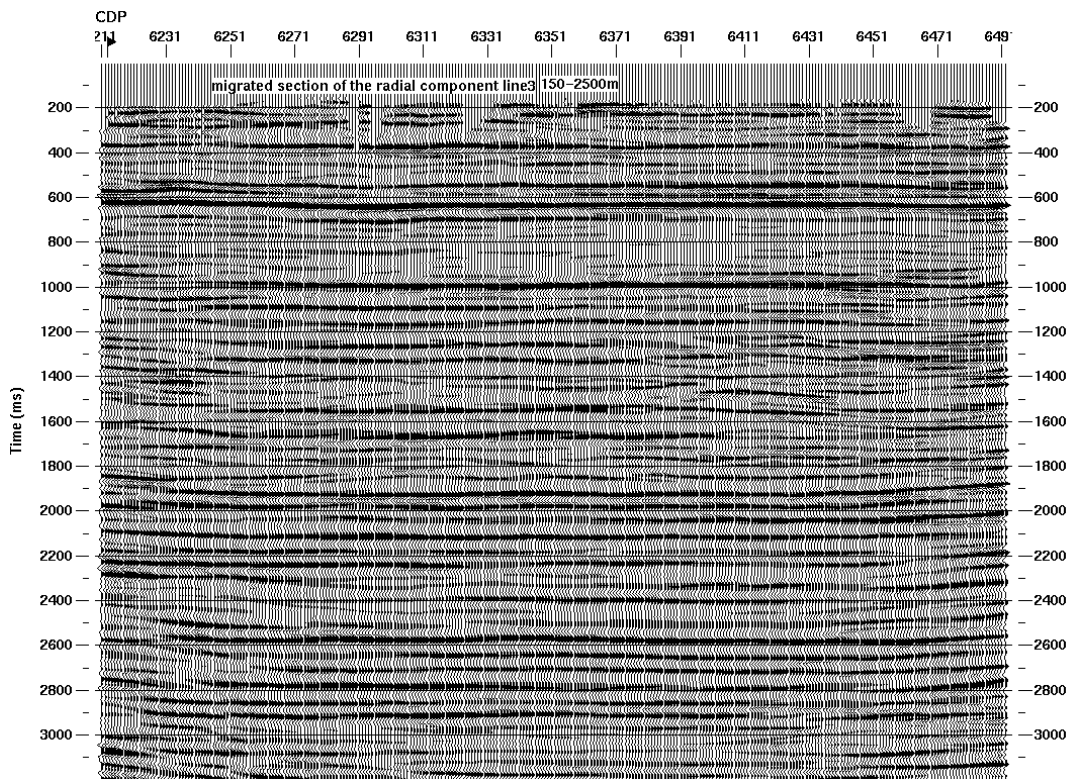FIG. 10a. Line 2; Final migrated P-S section.

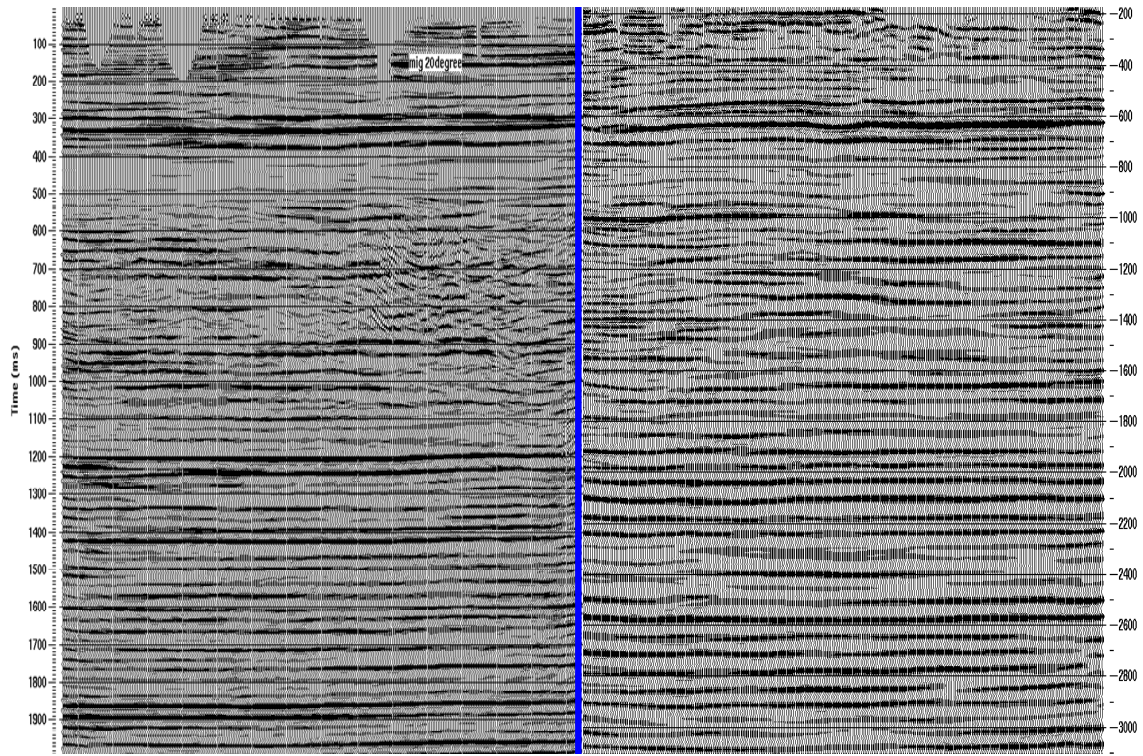FIG. 10b. Line 3; Final migrated P-S section.

FIG. 11a. Line 2; Comparison of P-P (left) and P-S (right) migrated sections. P-S section stretched to P-P time assuming V_P/V_S = 2.0
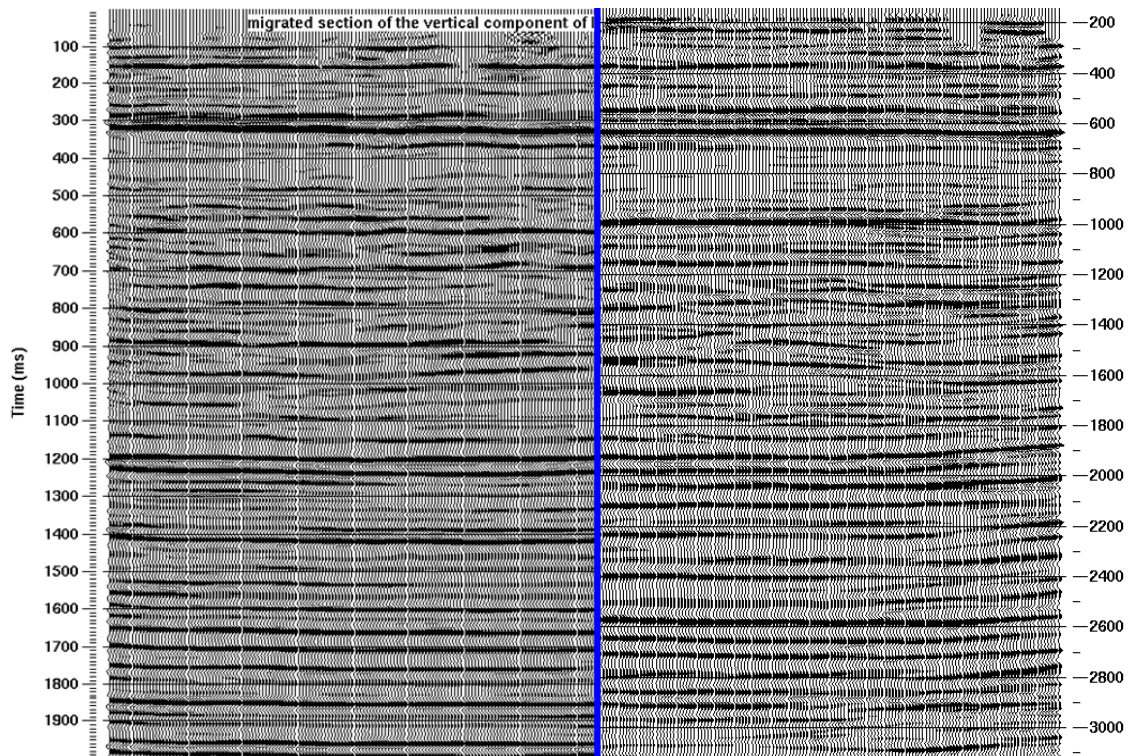

FIG 11b. Line 3; Comparison of P-P (left) and P-S (right) migrated sections. P-S section stretched to P-P time assuming V_P/V_S = 2.0
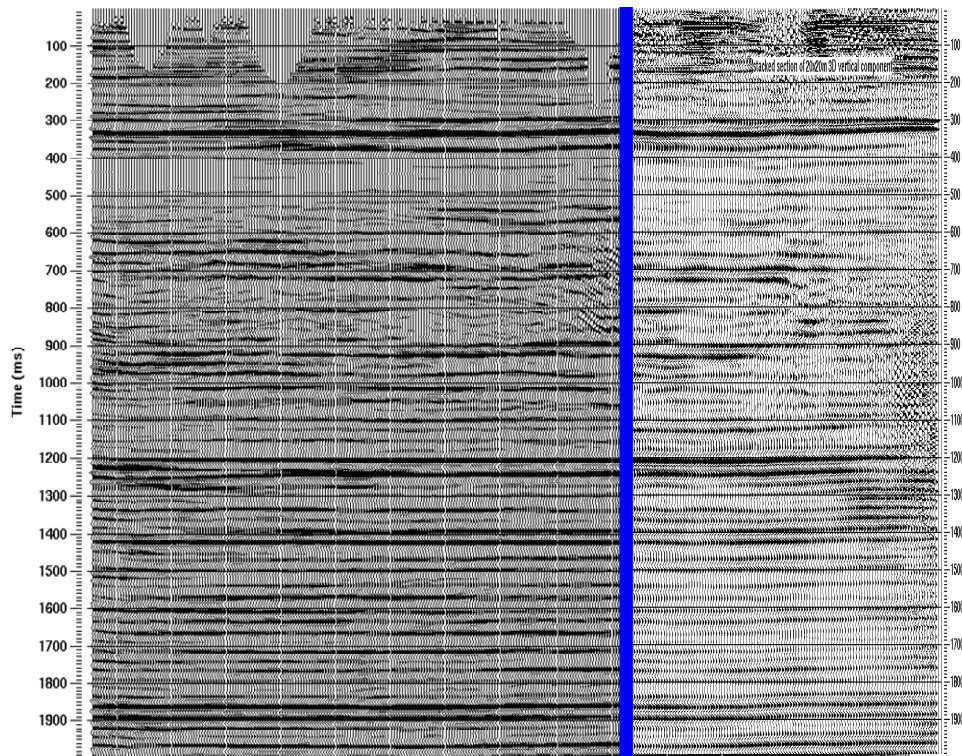
FIG. 12. Comparison of migrated P-P sections from Line 2 (left) and in-line 69 from Lu et al., 2005 (right).
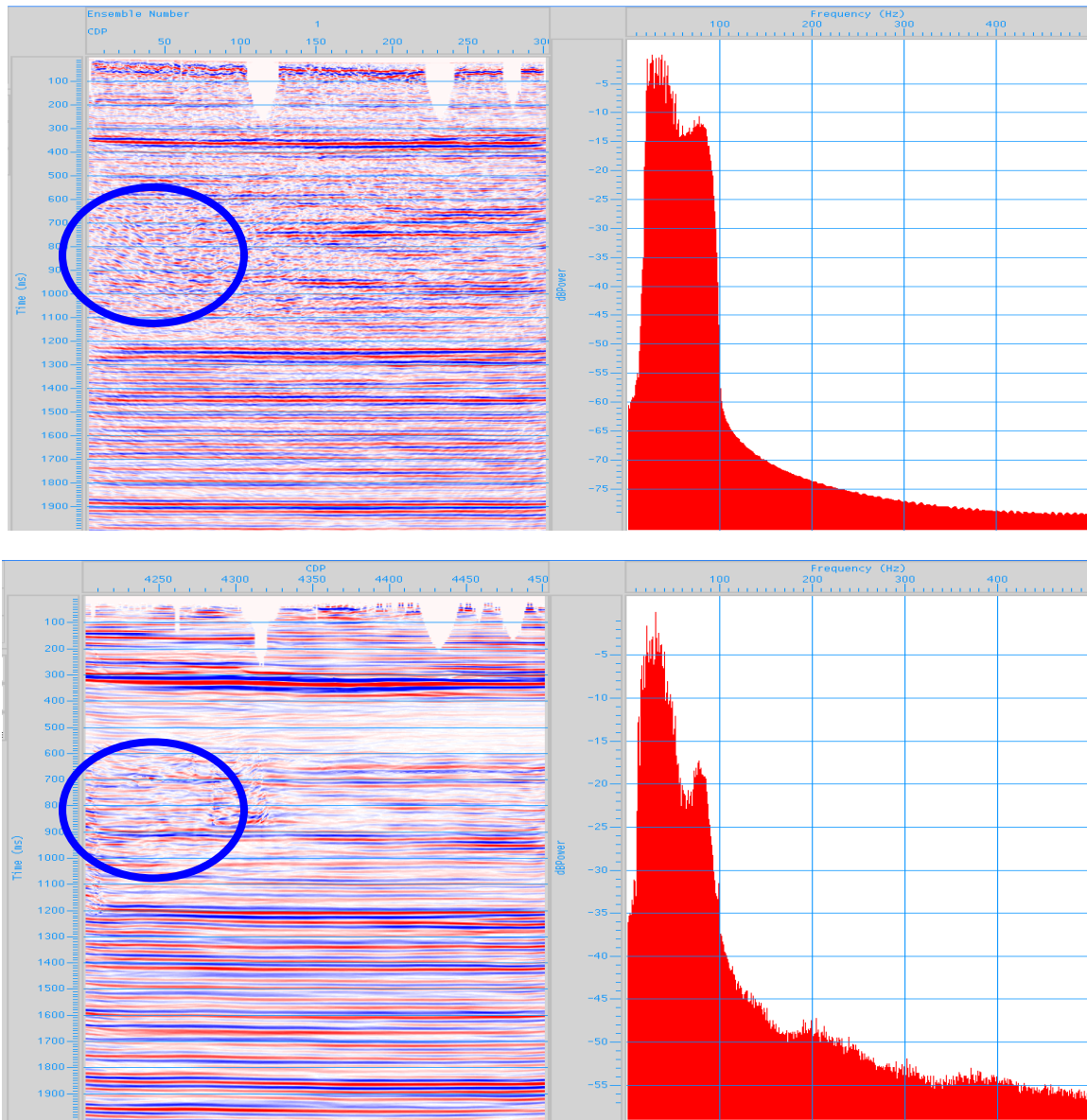
FIG. 13. Line 2; Vertical component migrated section from Veritas (top) and from CREWES (bottom). These sections have been band-pass filtered for comparison.

DISCUSSION

Data quality is high, and the vertical component processing of Lines 2 and 3 are very comparable to the equivalent in-lines from the 3D volume, as well as to contractor results. Radial component processing has also produced some very encouraging results.

ACKNOWLEDGEMENTS

REFERENCES

Lawton, D. C., Couëslan, M. L., Chen, F., Bland, H. C., Jones, M., Gallant, E. V., Bertram, M. B., 2005, Overview of the Violet Grove CO2 injection monitoring project: CREWES Research Report, **17**.

Lu, H., and Margrave, G. F., 1998, Reprocessing the Blackfoot 3C-3D seismic data: CREWES Research Report, **10**.

Lu, H., and Hall, K. W., 2003, Tutorial: Converted-wave (2D PS) processing: CREWES Research Report, **15**.

Lu, Hall, K.W., and Lawton, D.C., 2005, Violet Grove 2D and 3D data processing at CREWES: CREWES Research Report, **17.**